Indian Journal of
Applied Radiology

Open Science Publications

Volume 7, Issue 1 - 2021

www.opensciencepublications.com

Utility of Advance MR Imaging in Differentiation of Benign and Malignant Orbital Masses

Research Article

Bansal A[1], Kumar A[1]*, Bhatia V[1], Singh U[2], Ahuja CK[1] and Nahar U[3]

[1]*Department of Radiodiagnosis and Imaging, PGIMER, India*

[2]*Department of Opthalmology, PGIMER, India*

[3]*Department of Histopathology, PGIMER, India*

***Corresponding author:** Kumar A, Department of Radiodiagnosis and Imaging, PGIMER, Chandigarh - 160012, India, Phone: +91-7087009385; E-mail: ajay2509@gmail.com

Article Information: **Submission: 17/08/2021; Accepted: 10/11/2021; Published: 15/11/2021**

Abstract

Aim: The purpose of this study was to evaluate the utility of advanced MR techniques to improve the diagnostic ability to differentiate between these entities.

Material and Methods: A prospective evaluation of 26 patients (12 men and 14 women with a mean age of 34.8 years) presenting with orbital masses to our institute was done. MRI was performed in all patients with advanced techniques DWI, MRS and dynamic (DCE) on a 1.5 T scanner.

Results: ADC cut off value of 0.809 x 10-3 mm2/sec was determined using the ROC curve to differentiate malignant from benign lesions resulting in a sensitivity of 72.2% specificity of 75%, positive predictive value of 86.6% and Negative predictive value of 54.5%. Lesions with Tp < 141.5s showed a sensitivity of ~94.4% and specificity of ~87.5%, positive predictive value of 94.4% and Negative predictive value of 87.5%for malignancy. The lesions with Slope > 0.47 showed a sensitivity of ~100% and specificity of ~78%, positive predictive value of 66.6% and Negative predictive value of 100% for malignancy. Significant difference was seen between type I and type III curves with a p value ~0.002. Presence of choline peak had a sensitivity of ~ 62.5%, specificity of ~94.4%, positive predictive value of 83.3% and negative predictive value of 85% for malignancy.

Conclusion: Use of advanced MR imaging with inclusion of DW, MRS and perfusion parameters can significantly increase our diagnostic confidence in differentiating benign from malignant orbital lesions.

Introduction

Lesions in the orbit can be classified either according to the location of the mass or its histological subtype [1,2]. Conventional imaging techniques i.e. Multidetector computed tomography (MDCT) and magnetic resonance imaging (MRI) do not have sufficient sensitivity and specificity to help in differentiating malignant masses from benign lesions, with a high chance of misdiagnosis in case of unexpected rare entities [3,4]. Addition of new MR imaging techniques, like dynamic contrast enhanced (DCE) MR sequences, diffusion weighted imaging (DWI) and magnetic resonance spectroscopy (MRS), to the original sequences can provide different forms of tissue contrast and may help in better characterization of orbital lesions [5].

Methods

This was a single institution prospective study which was approved by the Ethics Committee of the institute. A total of 26 patients with orbital mass (12 men and 14 women with a mean age of 34.8 years) were enrolled over a period of one year in the study. These patients had come to our institute with complaints of proptosis and/or reduced visual acuity. The exclusion criteria for this study were contraindication for performing MRI study i.e. metallic implants, claustrophobia, and refusal to give consent and presence of large amounts of necrosis or calcification in orbital mass.

All studies were performed at 1.5T MRI unit (Siemens, Magnetom

ISSN: 2581-3919

Aera; Siemens Healthcare, Erlangen, Germany) equipped with high performance gradient system with a head coil with the following protocol (Table 1). All the imaging data was systematically evaluated by two radiologists (one fellow resident and second neuro radiologist with over 10 years of experience).

For DWI, all regions of interests (ROIs) were drawn manually. ADC values were calculated by adjusting the size of the ROI according to the size of the lesion. In lesions less than 2 cm in maximum diameter, one ROI was taken of .014 sq cm areas. In lesions that were larger than 2 cm, at least two or more ROIs were placed, avoiding the necrotic component of the lesion, and their mean (ADC_{mean}) values calculated. The ADC values were expressed in 10^{-3} mm^2/s. For MRS, Chemical shift imaging (CSI), using multiple voxels, or single voxel spectroscopy (SVS) was used according to size of the lesion and morphological appearance. Water and fat suppression was done automatically prior to all spectroscopic examinations using CHESS and other volume fat suppression techniques. For DCE, a coronal dataset including the lesion was acquired just before injection of the contrast and subsequently 6 datasets were acquired in a time period of 5 minutes after contrast injection. Multiple ROIs were applied and one ROI was selected which showed maximum enhancement pattern. The size of the lesion determined the size of the ROIs. The signal intensity (SI) of each slice of the dynamic sequence was determined from its mean pixel value. The representative ROI and corresponding time intensity curve (TIC) were obtained for each mass. -Three types of enhancement curves were obtained [4]: (i) The persistent pattern (type-I) - The lesion shows continuous progressive enhancement (ii) The plateau pattern (type-II) - In this pattern, there is a sharp rise in the enhancement, which then attains a plateau (iii) The washout pattern (type-III) - a rapid rise in enhancement followed by rapid decline with the final signal intensity <90% of the peak signal intensity. Each TIC was used to derive values for the baseline signal intensity (SI_{pre}), maximum signal intensity at the peak of enhancement (SI_{max}), and times corresponding to these signal intensities (T_{pre}, T_{peak}).Dependent parameters like peak enhancement (PH), enhancement ratio (ER_{max}) and Slopemax, were calculated using the above mentioned four independent variables with the help of the following formulas

- $PH = SI_{max} - SI_{pre}$
- $ER_{max} = \left(SI_{max} - SI_{pre}\right) / SI_{pre} \times 100$
- $Slope_{max} = \left(SI_{max} - SI_{pre}\right) / \left[SI_{pre} \times \left(T_{peak} - T_{pre}\right)\right] \times 100$

Final diagnosis was achieved in all cases through histopathological examination after the MR imaging.

Statistical analysis: Discrete categorical data (sex, MRS, Biopsy) was represented in the form of either a number or a percentage (%); Continuous data that were not normally distributed were reported as median and Inter quartile ranges. The distribution of the variables was tested with the Shapiro-Wilk test. For medians of ADC_{mean}, group comparisons (groups were Biopsy positive/negative) were made with the help of Mann Whitney test. Comparison of means of 2 groups of SI_{max}, Tp,PH, ER, Slope of the subjects was done using Independent t-test. To assess the performance of MRS in predicting the disease, sensitivity (Se), specificity (Sp), positive predictive value (PPV), negative predictive value (NPV) and diagnostic accuracy, keeping Biopsy as gold standard, were calculated using kappa test. Receiver operating characteristic (ROC) curves was calculated for SI (max), Tp, PH, ER, Slope and for ADC separately. Chi square or Fishers exact test was used to compare proportions which were dependent on their applicability. McNemar's test was used to see differences in diagnosis between two modalities. Concordance and discordance was calculated by method of Kappa test of agreement. All the statistical tests were two-sided performed at a significance level of α=.05. Analysis was conducted using IBM SPSS STATISTICS (version 22.0).

Results

The location of the masses is summarized in table 2: Of the 26 cases which were included in the study, 18/26 (69.2%) orbital masses were histopathologically proven to be benign and 8/26 (30.7%) malignant. The histopathological distribution is given in table 3. The means and standard deviations of ADC values of benign and malignant lesions were calculated separately and are shown in table 4. ROC was drawn and area under the curve (AUC) was determined as ~0.854 (Figure 1). A cut off value of 0.809 x 10-3 mm^2/sec was determined using the ROC curve to differentiate malignant from benign lesions resulting in a sensitivity of72.2% specificity of 75%, positive predictive value of 86.6% and Negative predictive value of 54.5%.

The DCE parameters of the benign and malignant lesions are summarized in table 5.

Out of these values Tp and Slope were found to have a significant difference between benign and malignant lesions. Tp had a p value of <0.001. ROC curve was drawn with the area under the curve 0.96 (Figure 2). A cut off value of 141.5 seconds was determined through the ROC curve and the lesions with Tp< 141.5s showed a sensitivity of ~94.4% and specificity of ~87.5% (Figure 2), positive predictive value of 94.4% and Negative predictive value of 87.5% for malignancy. Slope had a p value of <0.001. ROC curve was drawn with the area under the curve 0.889 and cut off value of 0.47 (Figure 3). Lesions with Slope > 0.47 showed a sensitivity of ~100% and specificity of ~78%, positive predictive value of 66.6% and Negative predictive value of 100% for malignancy.

Time intensity curves were plotted for perfusion parameters

Table 1: Showing the parameters used for MR acquisition.

	DWI	T1WI axial	T2WI axial	T2WI cor	T1W1 Pre and post contrast	DCE	PC T1WI
Sequence Type	Ep2d	Vibe_fs	Tse fs	Tse_fs	Mprage	Fl2d	Vibe_fs
TR/TE (ms)	3600/95	20/3.69	3000/89	4000/79	1800/3.77	175/2	20/3.69
Slice thickness (mm)	4.0	1.00	2.5	3.5	1.0	2.0	1.00
Acquired voxel size (mm3)	1.8 x 1.0 x 4.0	0.6 x 0.6 x 1	0.7 x 0.5 x 2.5	0.5 x 0.5 x 3.5	1.1 x 1.0 1.0	1.0 x 1.0 x 2	0.6 x 0.6 x 1
Flip angle	-	12	150	150	9	70	12

Citation: Bansal A, Kumar A, Bhatia V, Singh U, Ahuja CK, et al. Utility of Advance MR Imaging in Differentiation of Benign and Malignant Orbital Masses. Indian J Appl Radiol. 2021;7(1): 168.

(Table 6). All the lesions which demonstrated type I pattern were benign and all lesions demonstrating type III pattern were malignant [5,11]. Of the 10 lesions demonstrating type II curve, seven were benign and three malignant. The malignant lesions demonstrating type II curve were lymphoma, carcinoma NOS and one MPNST. A p value of ~0.002 was seen among type I and III curves. Significant difference between benign and malignant lesions was not seen using the values of SI(pre), SI(max), PH and ER.

MRS data of the patients was analyzed. The kappa value generated was 0.877 which implies almost perfect agreement of choline peak with malignancy (Table 7). With use of choline peak a sensitivity of ~ 62.5%, specificity of ~94.4%, positive predictive value of 83.3% and Negative predictive value of 85% for malignancy was obtained. Representative cases showing histopathological proven benign and

Table 2: Location of lesions in orbit.

Location	Number
Intraconal	12
Extraconal	9
Intra-extraconal	5

Table 3: Histopathological distribution of benign and malignant lesions.

Benign	
Schwannoma	4
Pleomorphic adenoma	3
Hemangioma	2
Fungal granulomas	2
Arteriovenous malformation	1
Basal cell adenoma	1
Optic nerve meningioma	1
Dermoid cyst	1
Low grade glioma	1
Cavernous lymphangioma	1
Neurogenic tumour (unspecified)*	1
Total	18
Malignant	
Squamous cell Carcinoma **	2
Lymphoma ***	2
Malignant peripheral nerve sheath tumour (MPNST)	2
Carcinoma NOS	1
Extramedullary myeloid tumour	1
Total	8

Table 4: Distribution of ADC (mean) (10^{-3} mm^2/sec) values of benign and malignant lesions.

Biopsy		N	Mean	Std. Deviation	Minimum	Maximum	p value
Benign	ADC(mean)	18	1.189	0.441	0.656	1.996	0.005
Malignant	ADC(mean)	8	0.713	0.114	0.542	0.870	

Table 5: Distribution of DCE parameters with their corresponding p values.

	Biopsy	N	Mean	Std. Deviation	p value
SI(pre)	Benign	18	324.60	86.31	0.868
	Malignant	8	331.45	114.84	
SI(max)	Benign	18	588.41	146.03	0.827
	Malignant	8	603.93	204.72	
Tp	Benign	18	241.28	67.12	<0.001
	Malignant	8	118.25	32.2	
PH	Benign	18	263.81	125.88	0.541
	Malignant	8	272.51	97.66	
ER	Benign	18	86.8%	45.7%	0.826
	Malignant	8	83.1%	17.7%	
Slope	Benign	18	0.36	.17	<0.001
	Malignant	8	0.75	.32	

Table 6: Number of lesions showing different types of enhancement curves.

TIC	Benign	Malignant
Type I	11	0
Type II	7	3
Type III	0	5

Table 7: Kappa test of agreement between MRS and histopathology.

		Value	Asymp. Std. Error(a)	Approx. T(b)	Approx. Sig.
Measure of Agreement	Kappa	.612	.173	3.181	.001
N of Valid Cases		26			

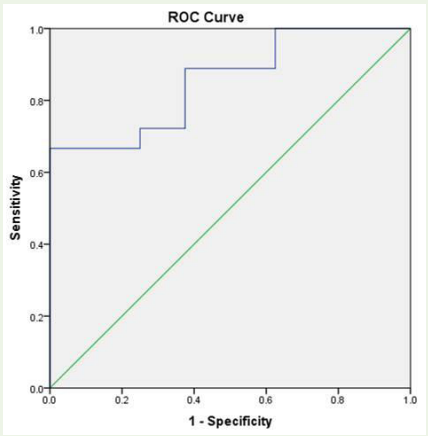

Figure 1: ROC curve for ADC (mean).

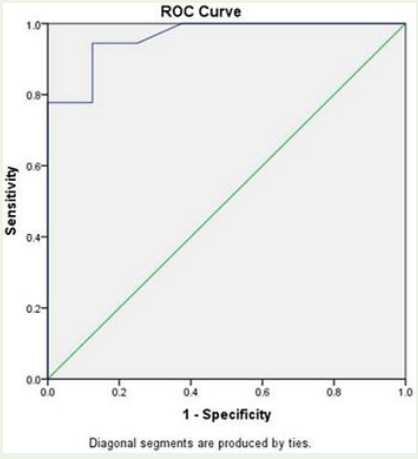

Figure 2: ROC curve for Tp.

Citation: Bansal A, Kumar A, Bhatia V, Singh U, Ahuja CK, et al. Utility of Advance MR Imaging in Differentiation of Benign and Malignant Orbital Masses. Indian J Appl Radiol. 2021;7(1): 168.

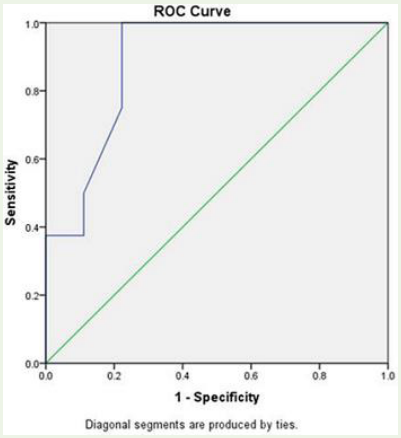

Figure 3: ROC curve for Slope.

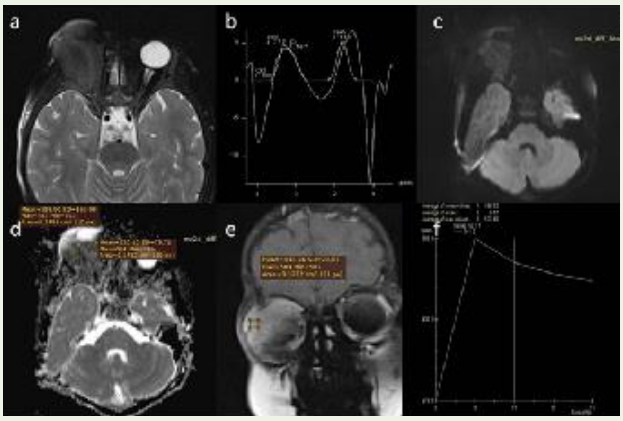

Figure 4: A 5 year old male child with massive proptosis showing a T2 isointense lesion (a) in the intra and extraconal compartment which is encasing and compressing the eyeball and the optic nerve. It is showing a choline peak on MRS (b) and diffusion restriction with an ADC mean of 0.542 x 10-3 mm2/sec (c) and (d). DCE curve was a type III curve with final SI <90% of SI max (e) and (f). Histopathological analysis revealed extramedullary myeloid tumor.

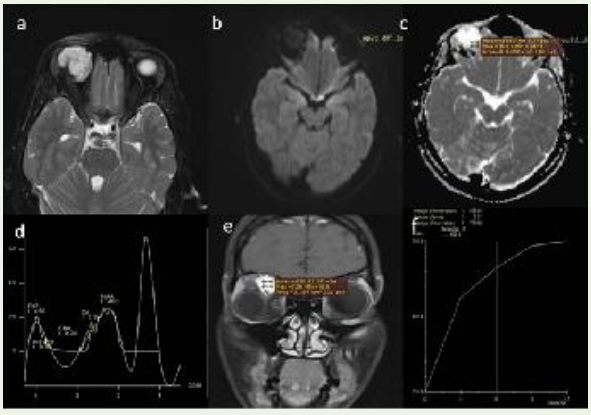

Figure 5: A 19 year old female with histopathologically proven cavernous hemangioma. (T2 weighted axial image (a) shows T2 hyperintense lesion in the intra and extra conal compartment which is showing only few areas of diffusion restricton (b). The ROI for ADC map was taken from the solid appearing lesion showing minimal diffusion restriction (b,c). No choline was peak on MRS (d) and DCE showed persistent pattern of enhancement. (e,f).

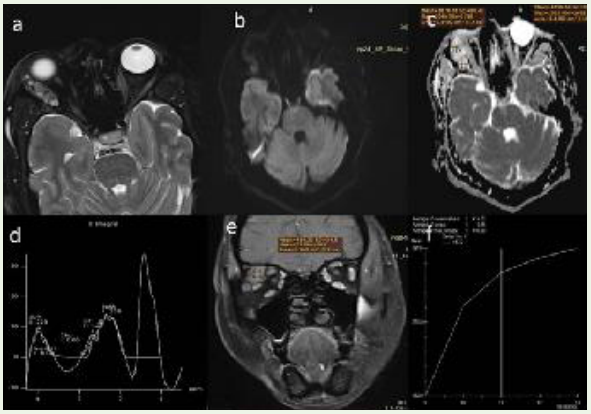

Figure 6: A 48 year old female presenting with pain and swelling in the right eye. (a) T2 weighted axial image of the orbit showing heterogeneously T2 hyperintense lesion which on (b) and (c) is not showing diffusion restriction. No choline peak is seen on MRS (d) and DCE images shows a persistent curve (e) and (f). It was histologically proven to be pleomorphic adenoma.

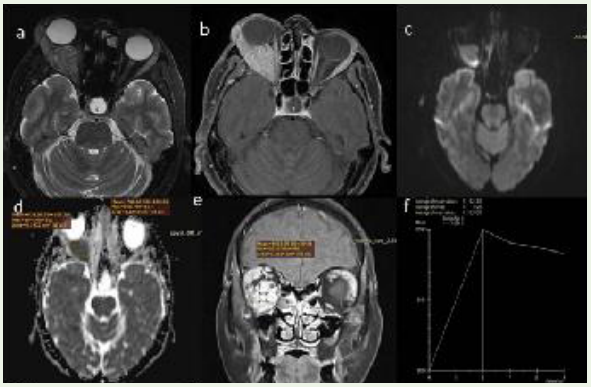

Figure 7: Histopathologically proven Non Hodgkins lymphoma in a 55 year old female.(a) A homogeneous T2 isointense intra and extraconal lesion in right orbit showing expansion of the intraconal space and showing homogeneous intense contrast enhancement (b). It is showing diffusion restriction (c,d,e,f) on DCE is showing a plateau cruve (final SI is >90% of SImax).

malignant orbital mass evaluated with above parameters are shown in figures 4-7.

Discussion

There is a need to differentiate between benign and malignant orbital masses for better treatment planning of individual cases [6,7,8]. A study conducted by Ben Simon et al., showed poor sensitivity of both CT and MR features in differentiation of malignant from benignlesions [9].

In our study, we applied newer MRI sequences DWI, DCE-MRI and MRS to evaluate few objective criteria to differentiate the nature of the lesions. On histopathological evaluation, 69.2% (18) lesions in our study were benign and 30.7 (eight) malignant, which roughly corresponds to the ratio in the general population [2].

Malignant tumors have increased cellularity with large nuclei and reduced extra-cellular space, which leads to restriction of free water movement and a dark signal on ADC map [10]. Sepahdari et al. found

Citation: Bansal A, Kumar A, Bhatia V, Singh U, Ahuja CK, et al. Utility of Advance MR Imaging in Differentiation of Benign and Malignant Orbital Masses. Indian J Appl Radiol. 2021;7(1): 168.

that benign lesions had a higher ADC value than malignant A cut off value of 1.0 x 10^{-3} mm^2/sec was determined [5], which resulted in a sensitivity of 63%, specificity of 84% and accuracy of 71% for differentiating benign vs malignant lesion. Similar studies were done by Razek et al. and Fatima et al. [11,12], demonstrating the usefulness of ADC mapping in differentiating benign from malignant lesions.

In our study, cut off value of 0.809 x 10^{-3} mm^2/sec was generated having a sensitivity of 72.2% and specificity of 75%. The PPV generated was 86.6% and NPV 54.4%. Therefore, although the sensitivity and specificity of ADC values is relatively low, this test has a high positive predictive value for benign lesions having ADC value of > 0.809 x 10-3 mm^2/sec. A significantly low ADC value (0.656 x 10-3 mm2/sec) was seen in a benign lesion which was proven to be meningioma on histopathology, which can be explained by the high cellularity of meningiomas.

DCE-MRI assesses the nature of the enhancement of the lesion against time which helps in evaluating the microcirculation of the lesion [6,13]. Xian et al. performed DCE-MRI on orbital lesions and concluded that a washout type TIC was the most predictive for malignancy [3]. A Study was done by Yuan et al. that all the lesions with a persistent pattern of enhancement (type I) curve turned out to be benign and 10 out of 14 lesions were showing type III curve were malignant [13]. Malignant lesions were found to have statistically higher Out of all the parameters, highest sensitivity (93.8%) was provided by Slope when the cut off value used was 1.10 while highest specificity (87.5%). was provided by a cut off value of 35.14 secs for Tp.

We found significant difference between type I and type III curves (p value ~0.002). All lesions demonstrating type I curve were benign (eight) and seven benign lesions also demonstrated type II curve. This can be attributed to the fact that benign lesions generally have an intact microvasculature which has limited permeability.

Tp was the most optimal with the value of 0.96with the highest specificity of 87.5% (with a cut off value of 141.5 secs). The corresponding sensitivity generated was 94.4%, PPV was 94.7% and NPV 87.5%. This signifies a high diagnostic accuracy of this test to differentiate benign and malignant orbital masses. The maximum sensitivity (100%) was obtained from slope with a cut off value of 0.47, however the corresponding specificity was relatively low (78%). The corresponding PPV and NPV were 66.6% and 100%. Values may also differ from previous studies as the values are calculated by drawing ROIs, the method of which can be different for different studies.

MRS has been shown to be useful to distinguish pure tumors from spectroscopically normal tissues [14,15]. Roshdy et al. showed choline peak in all (100%) patients with malignancy, and also in 14% of benign lesions, both of which were found to be optic nerve glioma [16]. In our study kappa test of agreement was applied to correlate MRS with histopathological diagnosis and the K value generated for choline peak was 0.612 which denotes a good level of agreement between spectroscopy and histopathology. The sensitivity of this test was low (62.5%) however specificity was 94.4% and the test had high PPV and NPV which suggests that presence of a choline peak was a significant sign of malignancy. The major limitation of MRS in orbit is the presence of blood, bone and fat surrounding the lesion which may lead to artefacts which was mitigated by taking single voxel spectroscopy in smaller lesions and chemical shift imaging in larger lesions. For a diagnostic test to accurately diagnose malignant lesions, the specificity should be 100% which was only attained by MRS. (Tp had the next highest specificity of 87.5%). All the three modalities can be used complementary to each other in addition to the conventional sequences to increase the confidence of diagnosing malignant lesions and help to plan treatment.

One of the major limitations of our study is the small sample size which did not allow us to differentiate between the specific subtypes of malignant lesion. Another limitation is the use of ROIs in all the three sequences which are user dependent. However this limitation was mitigated in our study by taking multiple ROIs of fixed areas and taking mean values as the standard value. Further studies using a larger population group may be needed to establish the usefulness of these sequences in orbital masses and to differentiate different subtypes of masses.

Conclusion

Diffusion-weighted MRI using ADC (mean) can be used to differentiate between benign and malignant orbital masses. Out of the DCE parameters, only Time intensity curve, time to peak and Slope are useful in differentiating benign and malignant masses with Tp having a high specificity and Slope having a high sensitivity. Choline peak in spectroscopy shows high agreement with malignancy on histopathology. Combining these three sequences increases the confidence of predicting malignancy in an orbital lesion.

References

1. Tailor TD, Gupta D, Dalley RW, Keene CD, Anzai Y (2013) Orbital neoplasms in adults: clinical, radiologic, and pathologic review. Radiographics 33: 1739-1758.
2. Ro SR, Asbach P, Siebert E, Bertelmann E, Hamm B, Erb-Eigner K (2016) Characterization of orbital masses by multiparametric MRI. Eur J Radiol 85: 324-336.
3. Xian J, Zhang Z, Wang Z, Li J, Yang B, et al. (2010) Value of MR imaging in the differentiation of benign and malignant orbital tumors in adults. Eur Radiol 20: 1692-1702.
4. Nemec SF, Peloschek P, Schmook MT, Krestan CR, Hauff W, et al. (2010) CT-MR image data fusion for computer-assisted navigated surgery of orbital tumors. Eur J Radiol 73: 224-229.
5. Sepahdari AR, Kapur R, Aakalu VK, Villablanca JP, Mafee MF (2012) Diffusion-weighted imaging of malignant ocular masses: initial results and directions for further study. AJNR Am J Neuroradiol 33: 314-319.
6. Kundu S, Chopra S, Verma A, Mahantshetty U, Engineer R, et al. (2012) Functional magnetic resonance imaging in cervical cancer: current evidence and future directions. J Cancer Res Ther 8: 11-18.
7. Morgan B, Thomas AL, Drevs J, Hennig J, Buchert M, et al. (2003) Dynamic contrast-enhanced magnetic resonance imaging as a biomarker for the pharmacological response of PTK787/ZK 222584, an inhibitor of the vascular endothelial growth factor receptor tyrosine kinases, in patients with advanced colorectal cancer and liver metastases: results from two phase I studies. J Clin Oncol 21: 3955-3964.
8. Warner MA, Weber AL, Jakobiec FA (1996) Benign and malignant tumors of the orbital cavity including the lacrimal gland. Neuroimaging Clin N Am 6: 123-142.

Citation: Bansal A, Kumar A, Bhatia V, Singh U, Ahuja CK, et al. Utility of Advance MR Imaging in Differentiation of Benign and Malignant Orbital Masses. Indian J Appl Radiol. 2021;7(1): 168.

9. Ben Simon GJ, Annunziata CC, Fink J, Villablanca P, McCann JD, et al (2005) Rethinking orbital imaging establishing guidelines for interpreting orbital imaging studies and evaluating their predictive value in patients with orbital tumors. Ophthalmology 112: 2196-2207.

10. Tsuruda JS, Chew WM, Moseley ME, Norman D (1990) Diffusion-weighted MR imaging of the brain: value of differentiating between extraaxial cysts and epidermoid tumors. AJR Am J Roentgenol 155: 1059-65.

11. Razek AA, Elkhamary S, Mousa A (2011) Differentiation between benign and malignant orbital tumors at 3-T diffusion MR-imaging. Neuroradiol 53: 517-522.

12. Fatima Z, Ichikawa T, Ishigame K, Motosugi U, Waqar AB, et al. (2014) Orbital masses: the usefulness of diffusion-weighted imaging in lesion categorization. Clin Neuroradiol 24: 129-134.

13. Yuan Y, Kuai XP, Chen XS, Tao XF (2013) Assessment of dynamic contrast-enhanced magnetic resonance imaging in the differentiation of malignant from benign orbital masses. Eur J Radiol 82: 1506-1511.

14. Hwang YF, Huang TY, Hwang SL, Kwan AL, Howng SL (2004) Differentiation among metastatic brain tumors, radiation necroses, and brain abscesses using proton magnetic resonance spectroscopy. Kaohsiung J Med Sci 20: 437-442.

15. Wang CK, Li CW, Hsieh TJ, Chien SH, Liu GC, et al. (2004) Characterization of bone and soft-tissue tumors with in vivo 1H MR spectroscopy: initial results. Radiology 232: 599-605.

16. Roshdy N, Shahin M, Kishk H, El-Khouly S, Mousa A, et al. (2010) Role of new magnetic resonance imaging modalities in diagnosis of orbital masses: a clinicopathologic correlation. Middle East Afr J Ophthalmol 17: 175-179.

Citation: Bansal A, Kumar A, Bhatia V, Singh U, Ahuja CK, et al. Utility of Advance MR Imaging in Differentiation of Benign and Malignant Orbital Masses. Indian J Appl Radiol. 2021;7(1): 168.